

UKSeaMap 2010 Technical Report 4

Energy

Fionnuala McBreen, Natalie Askew & Andrew Cameron

November 2011

© JNCC, Peterborough, 2011

For further information please contact:

Marine Ecosystems

[Joint Nature Conservation Committee](#)

Monkstone House, City Road

Peterborough, PE1 1JY, UK

jncc.defra.gov.uk/ukseamap

Contents

1	Introduction.....	1
1.1	UKSeaMap 2010 modelling approach	1
1.2	UKSeaMap 2010 energy	2
1.2.1	Wave disturbance.....	2
1.2.2	Seabed energy layers.....	2
2	Waves.....	3
2.1	Wave models.....	5
2.2	Wave disturbance.....	9
2.2.1	Wave disturbance threshold analysis.....	10
2.2.2	Wave disturbance confidence.....	10
2.3	Peak seabed kinetic wave energy	14
2.3.1	Peak seabed wave energy threshold analysis	14
2.3.2	Seabed kinetic wave energy confidence	26
3	Tidal currents	27
3.1	Tidal current models	27
3.2	Seabed kinetic current energy threshold analysis	28
3.3	Current energy confidence	30
4	Combined energy layer	31
5	Conclusions.....	32

Table of figures

Figure 1: Diagram showing the UKSeaMap 2010 process to predict seabed habitats and assess their confidence.....	2
Figure 2: Extent of wave models used.	5
Figure 3: 1 in 5 year significant wave height (Hs) from the NOC ProWAM model and the DHI Spectral Wave model. Classes are defined using natural breaks. See Table 1 for definition.	7
Figure 4: Wave period (Tp) from the NOC ProWAM model and the DHI Spectral Wave model. Classes are defined using natural breaks.	8
Figure 5: Peak seabed water velocities due to waves at the seabed. Classes are defined using natural breaks.....	9
Figure 6: Probability of wave disturbance.....	11
Figure 7: UKSeaMap 2010 map of wave disturbance showing where the seabed has a higher probability of being disturbed than being undisturbed.....	12
Figure 8: UKSeaMap 2006 map of wave disturbance.....	13
Figure 9: Wave exposure categories taken from the Location table in Marine Recorder for Orkney, Shetland and Northern Scotland.	16
Figure 10: Wave exposure categories taken from the Location table in Marine Recorder from the Minches and western Scotland.....	17
Figure 11: Wave exposure categories taken from the Location table in Marine Recorder of southern Scotland, northern England and Northern Ireland.....	18
Figure 12: Wave exposure categories taken from the Location table in Marine Recorder for eastern and southern England.	19
Figure 13: Wave exposure categories taken from the Location table in Marine Recorder of Wales and south-western England.....	20
Figure 14: Peak seabed wave kinetic energy (Nm ⁻²)	24
Figure 15: The relationship between energy class and wave exposure categories, shown as the percentage of sites located in each energy class (as shown in Figure 11) which have a particular wave exposure. ES = extremely sheltered, VS = Very sheltered, S = Sheltered, ME = Moderately exposed, E = Exposed, VE = Very exposed and EE = extremely exposed.	25
Figure 16: Extent of tidal models.	28
Figure 17: Classified map of peak seabed kinetic energy due to currents (for units see Table 11).	30
Figure 18: Classified map of combined peak seabed kinetic energy (due to both waves and currents).....	32

1 Introduction

1.1 UKSeaMap 2010 modelling approach

Classification of the seabed into habitat types was undertaken using geological, physical and hydrographic characteristics in a manner similar to that adopted in the UKSeaMap 2006 and MESH projects (Connor *et al*, 2006; Coltman *et al*, 2008). This approach recognises the strong correlation between environmental parameters and ecological character, such that mapping environmental parameters in an integrated manner can successfully be used to produce ecologically-relevant maps. UKSeaMap 2010 differs from previous broadscale modelling projects in that it takes account of uncertainty around boundaries in the classification of habitats, and includes this uncertainty as an element in a confidence map to accompany the habitat map.

Figure 1 shows the process employed by UKSeaMap 2010 to produce the predictive habitat map and confidence map. Numbered annotations are as follows:

1. In-situ biological data are used to establish the numeric values of physical parameters associated with boundaries between classes in the habitat classification system (e.g. between 'moderate energy' and 'high energy' classes).
2. In-situ physical data are used to assess variation between a physical data layer and a second source, such as independent in-situ measurements of the same parameter.
3. The variance of each physical data layer is then used to derive relationships between a given value of a grid cell and the probability that the value is within a class, relative to a single predefined boundary established in Step 1. These measurements of uncertainty therefore vary spatially across the physical data layer. It was not possible to carry out this step for the seabed substrata data layer. Through combining probability layers calculated in Step 2, the probability that a cell falls between two boundaries (defined in Step 1) that define the upper and lower bounds of a class can be calculated. This is the probability that the cell belongs to the class defined by those boundaries.
4. Comparing the probability that each cell belongs to each class is then achieved through a process of 'stacking' in GIS and the class with the highest probability is selected for each cell, resulting in classified physical data layers.
5. The classified physical data layers are combined in GIS, and interpreted with the habitat classification system to determine which habitats are represented by each combination of physical classes.
6. The probability associated with each 'winning' class that contributes to the final predicted habitat in each grid cell can then be taken as a measure of uncertainty in relation to the boundaries applied in the model.
7. Measurements of uncertainty at boundaries are combined with information about the quality of the physical data layers to produce a confidence map to accompany the habitat map. In UKSeaMap 2010 the seabed substrata data layer was the only layer assessed for quality (e.g. taking into account factors such as age, data density, data collection techniques). Confidence is therefore the interaction between how confident we can be that a habitat has been classified into the correct biological zone or energy class (which is caused by how clear or otherwise the boundaries are

between these zones or classes, and how good a predictor of any habitat these physical data are), and the quality of the information describing seabed substrata.

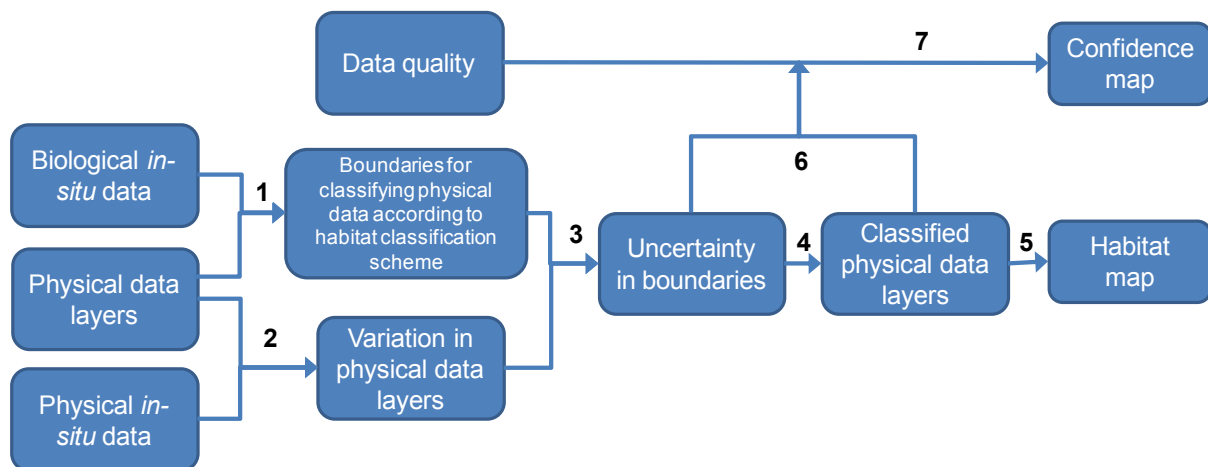


Figure 1: Diagram showing the UKSeaMap 2010 process to predict seabed habitats and assess their confidence

1.2 UKSeaMap 2010 energy

UKSeaMap 2010 used energy data in two ways. Wave disturbance was used to distinguish between the circalittoral and deep circalittoral biological zones, and seabed energy layers were used to distinguish between high, moderate and low energy categories for infralittoral and circalittoral rock.

1.2.1 Wave disturbance

The boundary between circalittoral and deep circalittoral biological zones is defined by the closure depth which is the maximum depth at which wave energy interacts with the seabed. The wave disturbance layers created for UKSeaMap 2010 were created under Task 1C of the MB0102 Defra data layers contract (Frost & Swift, 2010).

1.2.2 Seabed energy layers

In the EUNIS habitat classification scheme, energy is used at EUNIS Level 3 to classify infralittoral and circalittoral rock habitats into high, moderate and low energy environments. The energy classes are not applied to sediments because the sediment type itself is thought to reflect the hydrodynamic regime¹. Thus the focus is on the way rock is affected by seabed energy from waves and tidal currents. Full-coverage data for these variables were obtained through Task 2E of the Defra data contract MB0102 (West *et al*, 2010).

A number of variables can serve as measures of energy, and temporal resolution is an important issue to consider. Maximum wave energy structures habitats through its destructive powers, but a storm wave may only affect the seabed in a particular place every

¹ This relationship between sediment and energy is further explored in UKSeaMap 2010 Technical Report 5

10 or 20 years. Energy levels resulting from tidal currents on the seabed are a more constant force throughout the year.

Under Task 2E of the MB0102 Defra data layers contract (West *et al*, 2010), ABPmer produced two different types of seabed energy layers: bed shear stress and seabed kinetic energy. Bed shear stress takes account of friction at the seabed, which is calculated by using 'bed roughness' values, where different sediment types have different roughness lengths. Soulsby (1997) provides methods to calculate bed shear stress and the definitive list of sediment roughness values but the methods are derived based on sediment dynamics and does not provide a roughness value for rock. To create the bed shear stress layers in Task 2E, the maximum value for rippled sand was used as a proxy for rock. The results of this analysis were unsatisfactory in terms of the patterns that were produced around the UK. It is possible that the use of the rippled sand roughness value as a proxy for rock was causing some of these unexpected patterns. As a result, seabed kinetic energy was deemed to be a more appropriate measurement of energy on rock communities.

The seabed kinetic energy layers for waves and tidal currents, along with their confidence, are discussed in further detail in sections 2 and 3 respectively. This is followed by the process used to combine these layers to produce a single energy layer which could be used in the UKSeaMap 2010 modelling process (section 4).

2 Waves

The wave energy is divided into two main areas (as detailed above): wave disturbance and peak seabed kinetic energy due to waves.

Wave disturbance

Wave disturbance data was required to create the boundary between the circalittoral and deep circalittoral biological zones which is most often defined in the literature by the transition between disturbed and undisturbed areas of the seabed (from the effects of waves). Wave disturbance is used to delineate the boundary between the circalittoral (disturbed by waves) and deep circalittoral (undisturbed by waves) zones. This boundary is defined by the wave base: the point at which water depth becomes greater than half the wavelength as one moves from the circalittoral to the deep circalittoral. The wavelength is a function of wave period and water depth, with wavelength decreasing as the wave moves into shallower water..

Peak seabed kinetic energy layer due to waves

The peak seabed kinetic energy layer due to waves was required to create high, moderate and low energy classes which could be applied to EUNIS Level 3 rocky habitats. Data layers and associated confidence layers were required for each. The same wave models were used for both the wave disturbance and the seabed kinetic energy layers (see section 2.1). Table 1 provides definitions for terminology used in the wave sections.

Table 1: Definitions of wave parameters. Definitions taken from the National Oceanic and Atmospheric Administration's (NOAA) website and the Dictionary of Ecology.

Wave parameter	Definition
Wave crest	The highest part of a wave ² .
Wave trough	The lowest part of the wave ² .
Wavelength	Distance between crests or troughs of a wave ² .
Wave base	The depth beneath a water mass below which wave action ceases to disturb the sediments. Wave-base depth is approximately equal to half the wavelength of the surface waves. ³
Wave height	The distance from the wave trough to the wave crest ² .
Significant wave height	The average height (trough to crest) of the one-third highest waves valid for the indicated 6 hour period ⁴
Wave period	The time, in seconds, between the passage of consecutive wave crests past a fixed point ² .
Wave direction	The direction from which the waves are coming.
Wave steepness	The ratio of wave height to wavelength and is an indicator of wave stability. When wave steepness exceeds a 1/7 ratio; the wave typically becomes unstable and begins to break ² .
Swell waves	Wind-generated waves that have travelled out of their generating area. Swells characteristically exhibit smoother, more regular and uniform crests and a longer period than wind waves ² .
Wind waves	Local, short period waves generated from the action of wind on the water surface (as opposed to swell) ² .
Closure depth	The maximum depth at which wave energy interacts with the seabed (West <i>et al.</i> , 2010)

Aims

- Create a wave disturbance confidence layer to be incorporated in to the biological zones confidence layer
- Create a wave disturbance data layer showing areas of the seabed disturbed and undisturbed by waves to be used to distinguish the boundary between the circalittoral and Deep circalittoral zones.
- Create thresholds for high, moderate and low wave energy
- Create a confidence layer for peak seabed kinetic energy due to waves
- Create a classified peak seabed kinetic energy due to waves layer

² Definitions taken from NOAA's national weather service webpage: <http://www.weather.gov/glossary/index.php?letter=w>.

³ Dictionary of Ecology definition: <http://www.encyclopedia.com/doc/1O14-wavebase.html>

⁴ Definitions taken from NOAA's national weather service webpage: <http://www.nws.noaa.gov/forecasts/graphical/definitions/defineWaveHeight.html>

2.1 Wave models

The wave energy layers were built on data from the NOC⁵ ProWAM wave model (12.5 km resolution) and the DHI Spectral Wave model (100 – 300 m resolution) (West *et al.*, 2010) (Figure 2). The wave height and wave period parameters produced from these two wave models were combined. These parameters were then used to calculate peak seabed kinetic wave energy and wave disturbance layers.

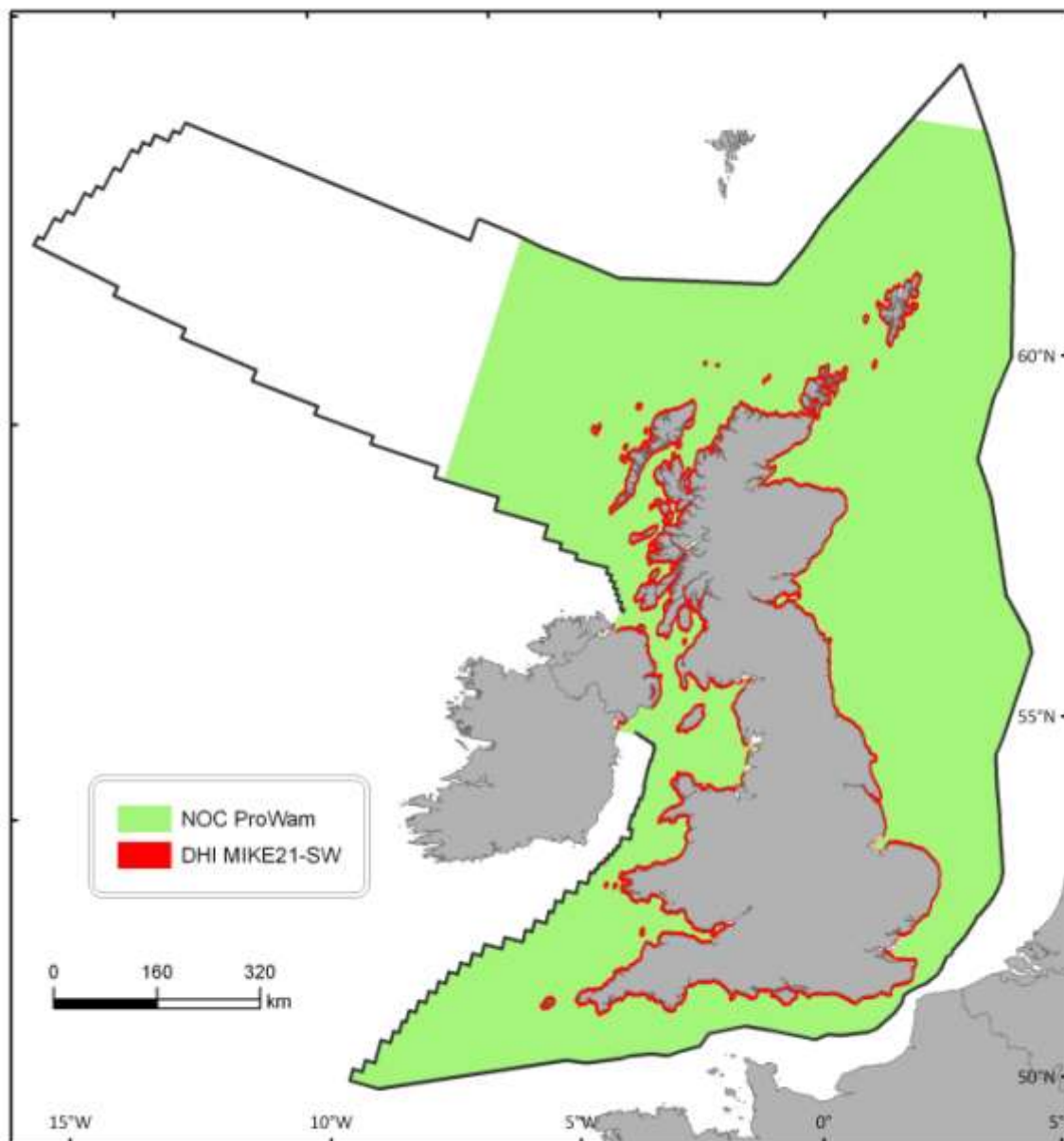


Figure 2: Extent of wave models used.

⁵ National Oceanographic Centre, formerly Proudman Oceanographic Laboratories (POL)

Data from the NOC ProWAM wave model covered the 5 year period from 2000 – 2004 and were based on 1 in 5 year peak values (i.e. the maximum value across all values for all 5 years, rather than an average of the maximum for each of the 5 years). These results were verified against field measurements and were filtered to remove swell waves (using wave steepness values with a ratio greater than 1/7) leaving only wind-wave results. Swell waves tend to have longer wave periods but shorter wave heights so they disturb the seabed less than wind waves.

The maximum wave for each NOC ProWAM grid cell was then determined to provide the 5 year extreme. These filtered, maximum wave heights (and their associated parameters – wave period and wave direction) were then used to define the boundary conditions for the Danish Hydraulic Institute's (DHI) MIKE21-SW (spectral wave) model. The DHI Spectral Wave model was used for areas within 6km of the coastline. Its inshore boundary was defined by Mean High Water Springs (MHWS). The offshore limit of this active wave zone was determined by the closure depth of the maximum annual wave (i.e. the depth at which a wave approaching the coastline begins to have a significant impact upon the seabed) which was found to be approximately 6 km. Bathymetry used as input to the DHI Spectral Wave model was derived from a combination of SeaZone and GEBCO bathymetric data. SeaZone data were used in preference to GEBCO where the two data sets overlapped (Technical Report No. 2). Where DHI Spectral Wave model and NOC ProWAM wave models overlapped, a cross-comparison of wave heights was made to ensure that the ABPmer model transformed an appropriate wave from the NOC ProWam model into the nearshore region.

Deep sea areas not covered by either model (areas located between 11°W and 24 °W – i.e. the Atlantic North West approaches and the north-east tip of UK marine area) were assumed to be areas where waves no longer exerted an effect on the seabed due to the depths involved. Wave disturbance and kinetic wave energy probability calculations were extended beyond the limit of ProWAM, as far as 24°W. Wave disturbance and kinetic wave energy probability calculations were extended beyond the limit of ProWAM, as far as 24°W, by inferring comparable values of wave period from the NOAA product Wavewatch III. The combined wave model used three parameters of wave direction, wave height and wave period (Figure 3 - Figure 4) to calculate the final wave energy layers.

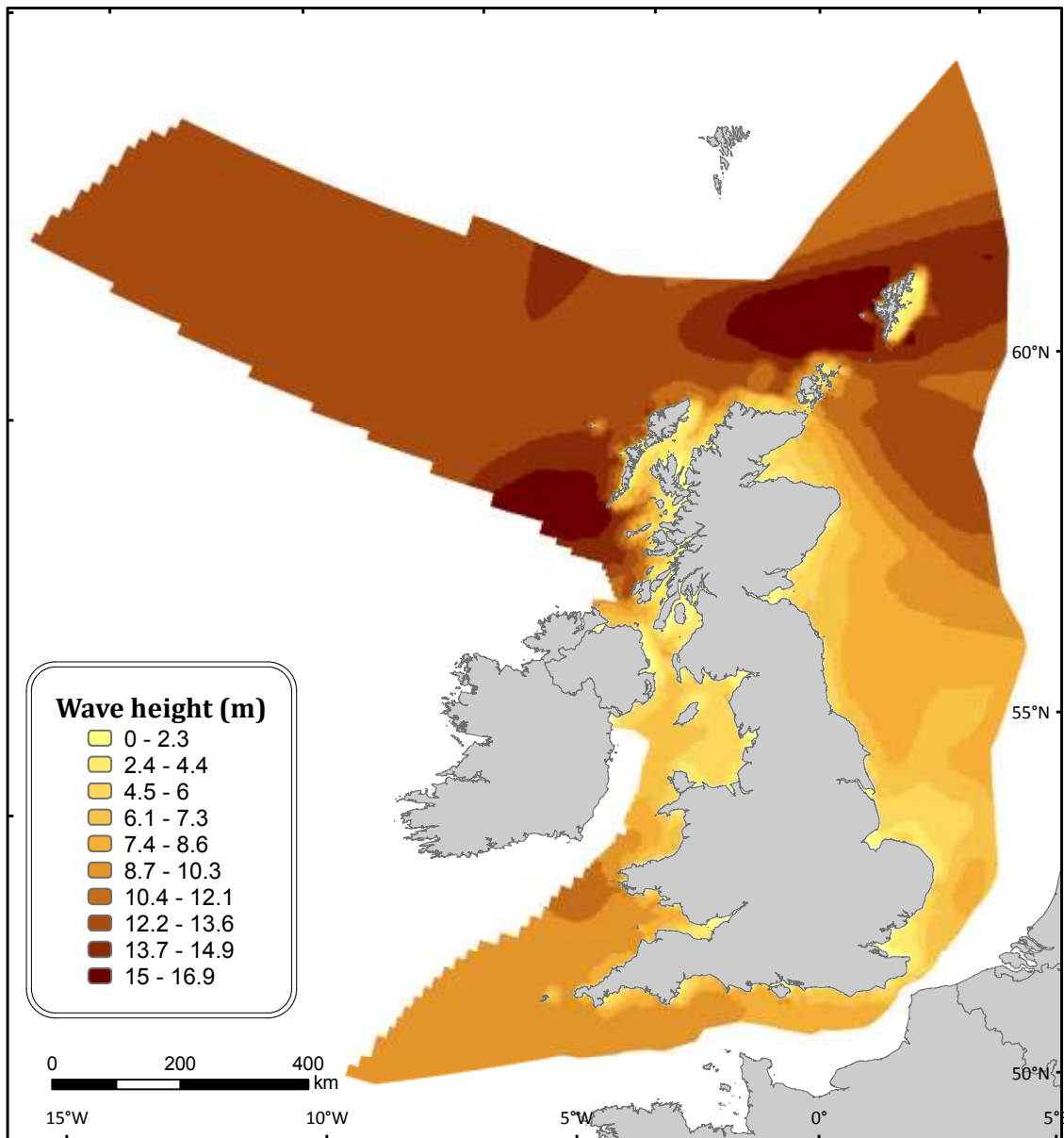


Figure 3: 1 in 5 year significant wave height (H_s) from the NOC ProWAM model and the DHI Spectral Wave model. Classes are defined using natural breaks. See Table 1 for definition.

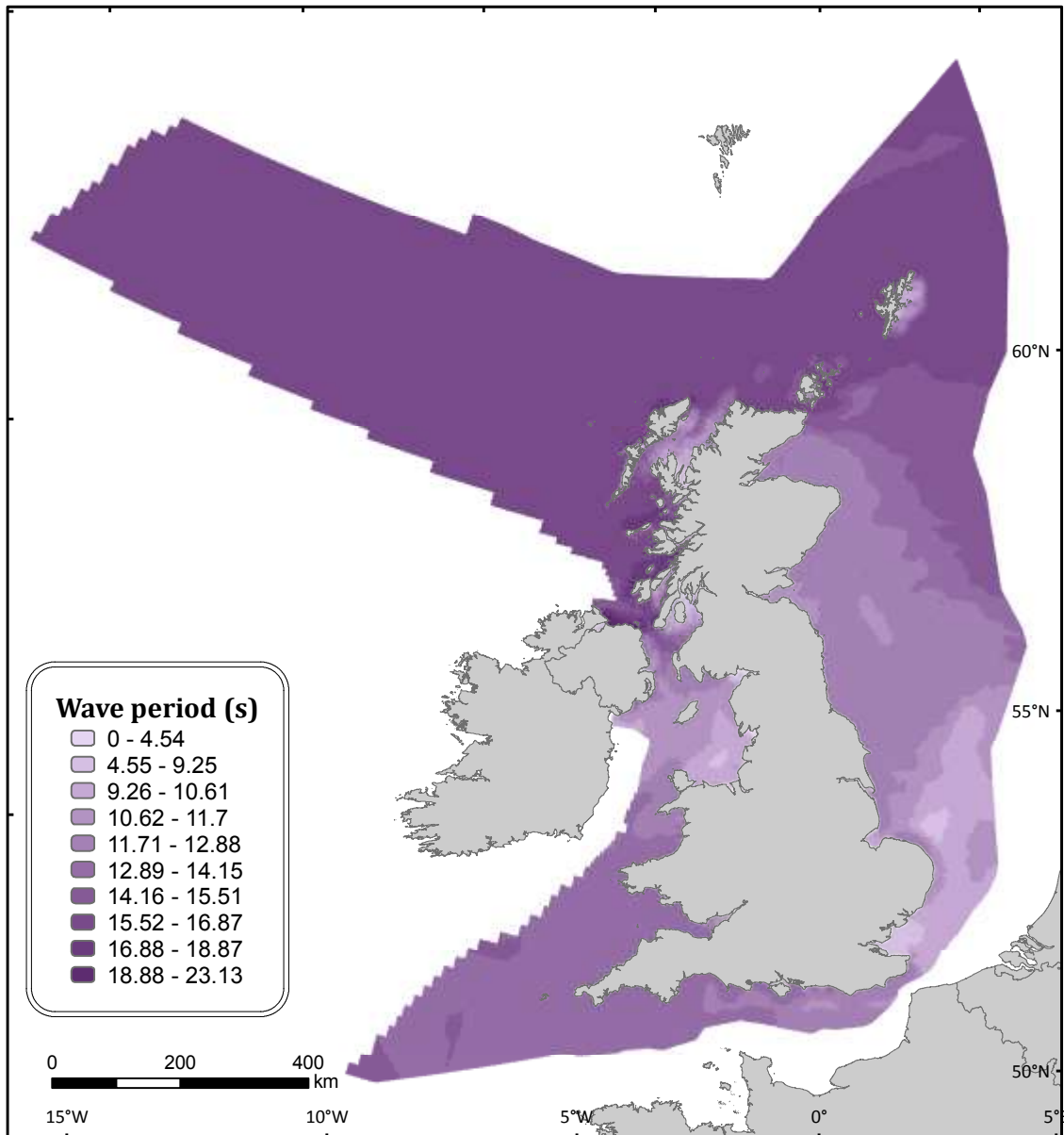


Figure 4: Wave period (T_p) from the NOC ProWAM model and the DHI Spectral Wave model. Classes are defined using natural breaks.

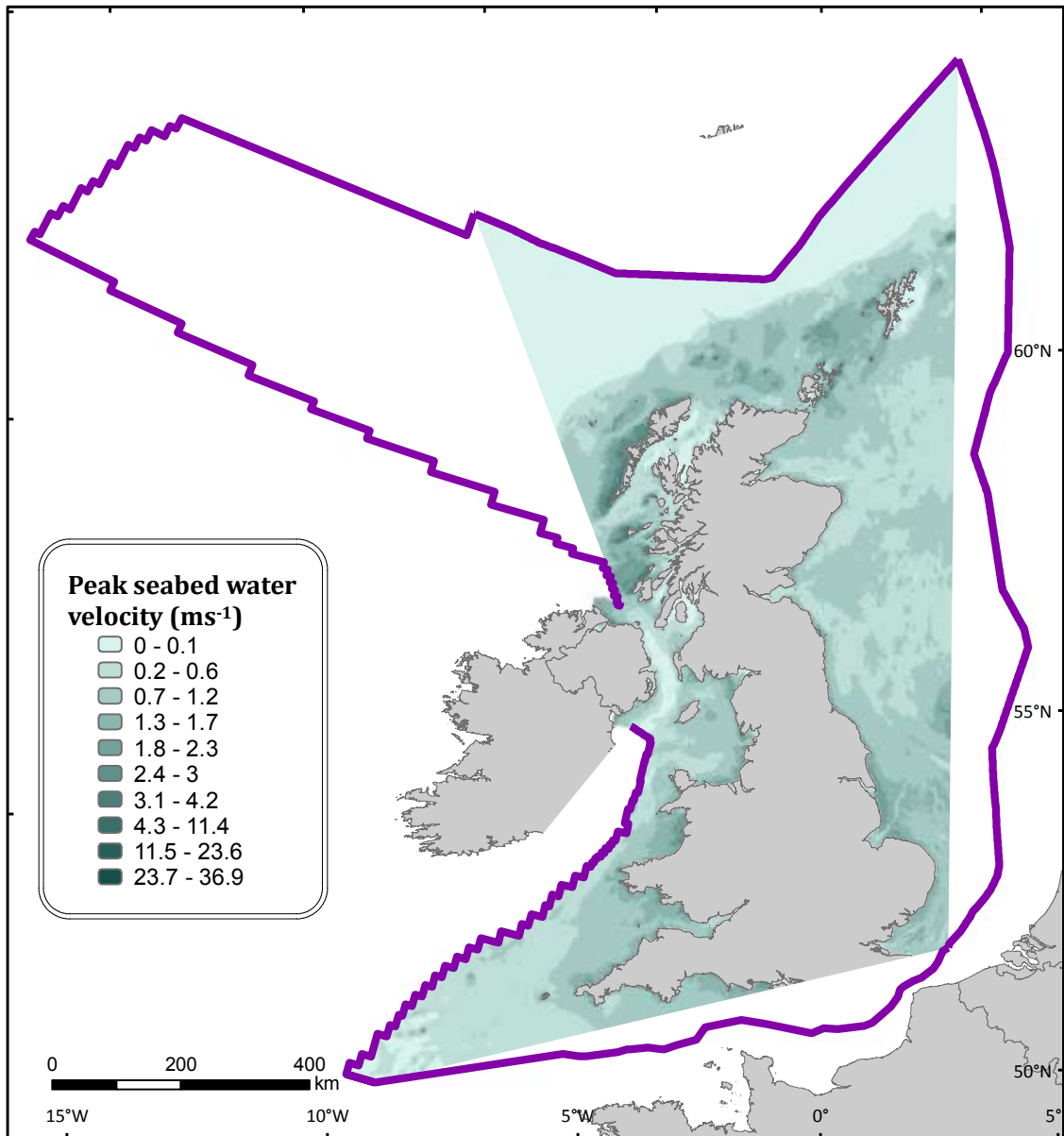


Figure 5: Peak seabed water velocities due to waves at the seabed. Classes are defined using natural breaks.

2.2 Wave disturbance

Wave periods from the NOC ProWam wave model and depths from the UKSeaMap 2010 bathymetry layer were used to calculate the corresponding wavelengths. The wave length layer is then used to produce a wave disturbance layer. The classification says the area undisturbed by waves is below the wavebase, thus by intersecting the wave length layer with a bathymetry layer the seabed which was at a depth less than or equal to $\frac{1}{2}$ the wave length was identified. This is the wave disturbance layer which was then used to delineate the lower limit of the deep circalittoral.

2.2.1 Wave disturbance threshold analysis

The threshold of the boundary between the circalittoral and deep circalittoral zones, which is defined by the closure depth, was not tested using habitat point data as there were not enough available habitat points in the deep circalittoral zone to test this boundary.

2.2.2 Wave disturbance confidence

The confidence of the wave model was assessed by evaluating time series of wave periods predicted by the NOC ProWam wave model against significant wave height and wave period field data from Cefas⁶ wave buoys. The Cefas WaveNet datasets consist of records from 93 post-recovery locations and 38 from telemetry sites.⁷ Of these 131 locations, 47 have data that fall within the temporal window offered by the proWAM wave model run. The confidence assessment looked at the mean and standard deviation of wave height and period values at corresponding time points of the NOC ProWAM wave model predictions and CEFAS wave buoy field data. The level of uncertainty in the predicted wave periods were derived and used to develop a corresponding probability distribution of wave lengths. The probability distribution of wave lengths was used to obtain a probability layer associated with predictions of wave disturbance of the seabed (Figure 6). (Frost & Swift, 2010).

The wave disturbance probability layer was used to define the wavebase shown in Figure 7. Figure 8 shows the wave disturbance map from the original UKSeaMap project (Connor *et al*, 2006). Disturbed areas appear to cover a larger area in the 2010 map, extending the circalittoral zone. Notable increases occur in the area between the Orkneys and the Shetlands and in the east and south east most likely due to the improved bathymetry dataset available for UKSeaMap 2010.

⁶ Centre for Environment, Fisheries and Aquaculture Science

⁷ Telemetry data is transmitted via radio or satellite signals. Post-recovery data is manually retrieved from the buoy.

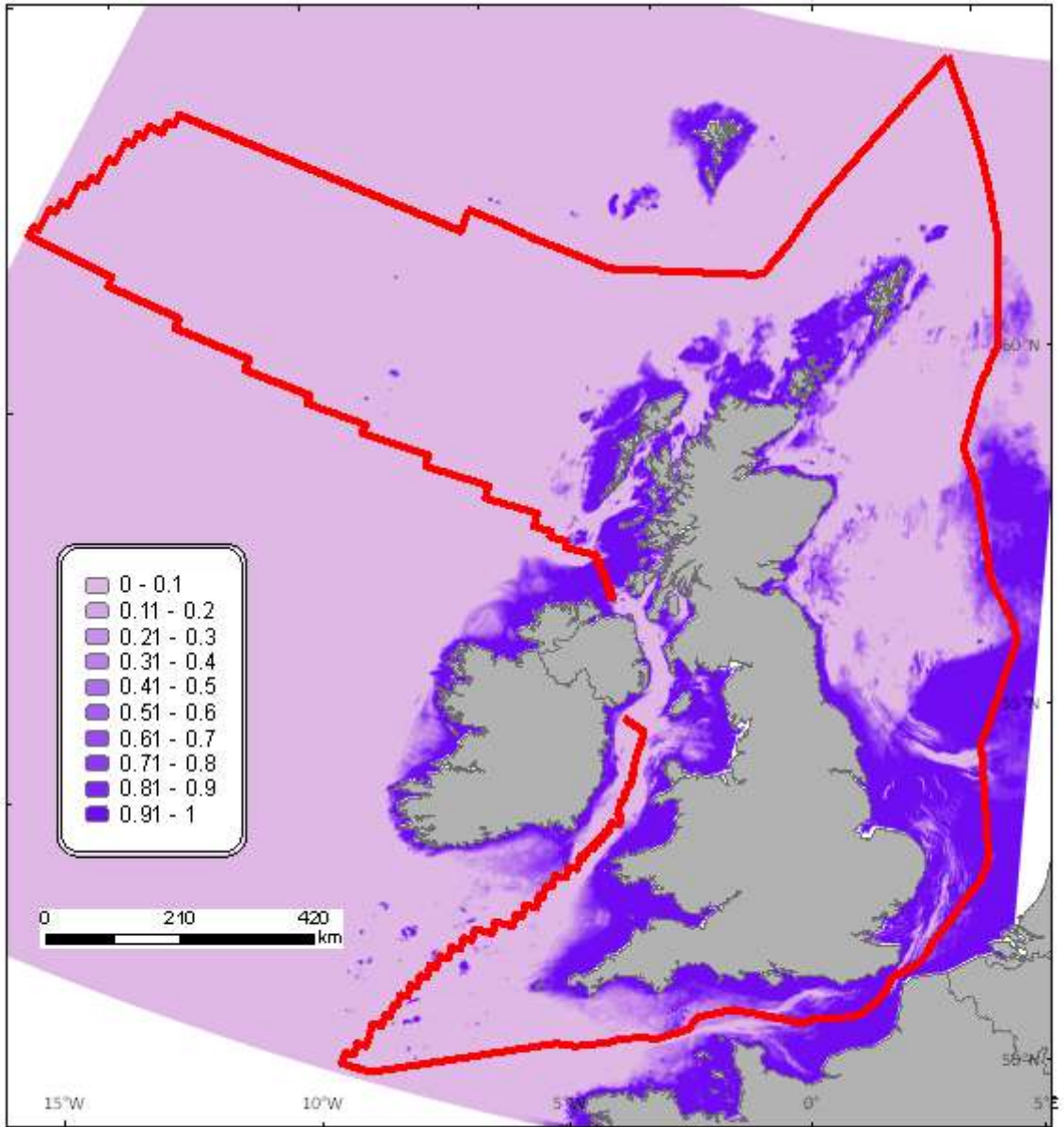


Figure 6: Probability of wave disturbance.

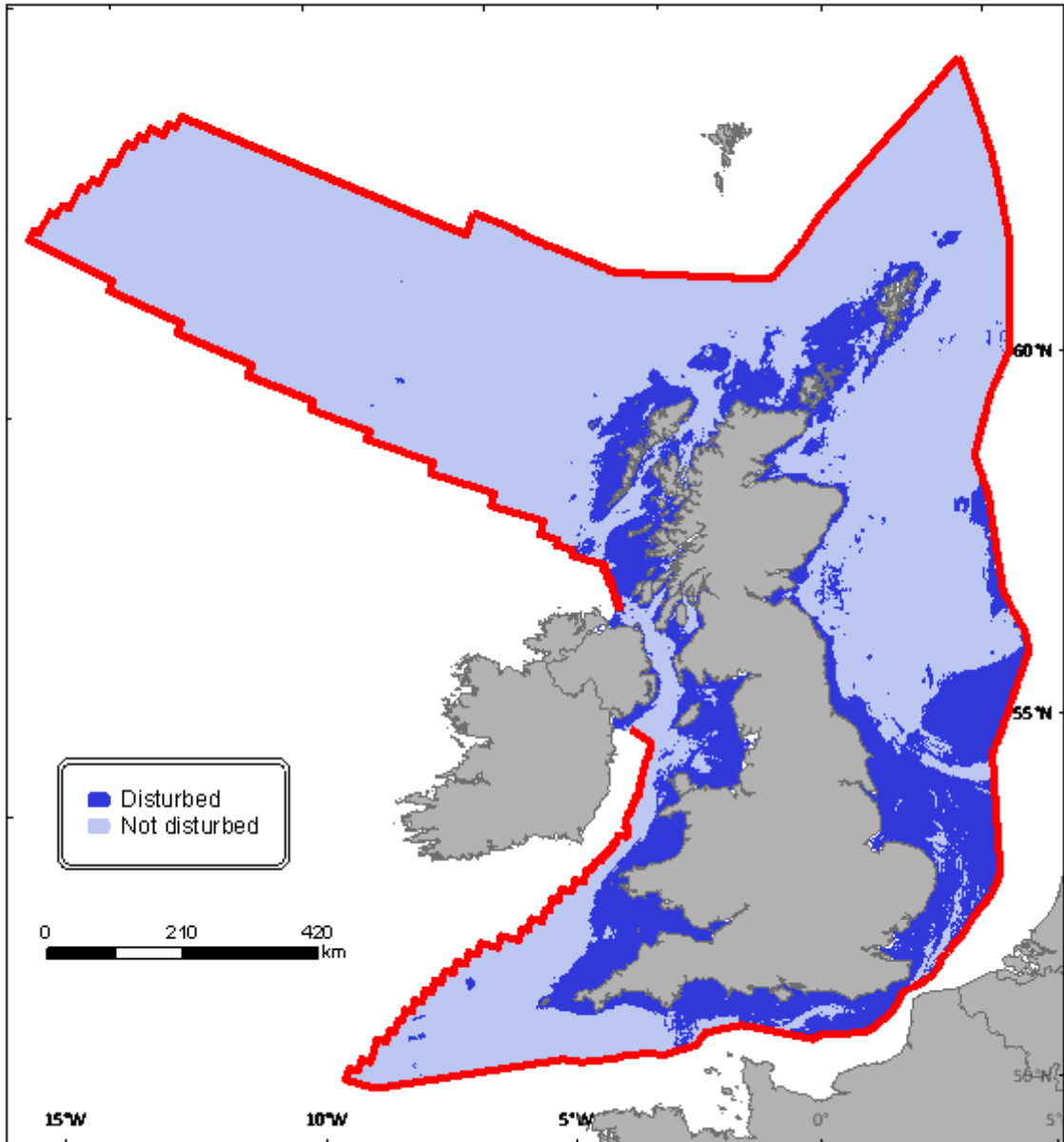


Figure 7: UKSeaMap 2010 map of wave disturbance showing where the seabed has a higher probability of being disturbed than being undisturbed.

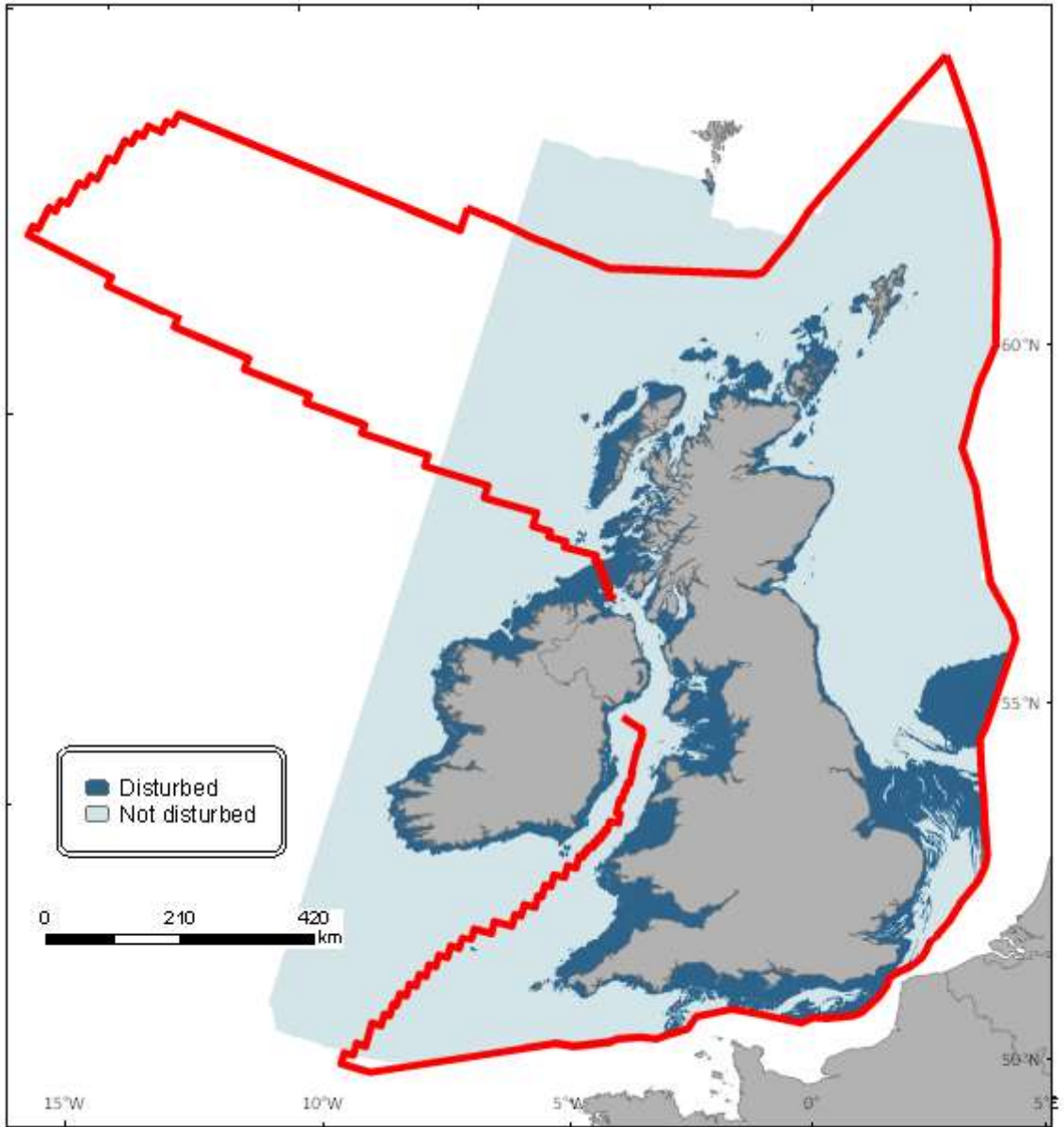


Figure 8: UKSeaMap 2006 map of wave disturbance.

2.3 Peak seabed kinetic wave energy

Peak seabed kinetic energy (KE) caused by waves was calculated using peak seabed water velocities (Figure 5) during a wave period (U_{wb}), using the formula $KE = \frac{1}{2} \rho U_{wb}^2$, where ρ is the density of seawater.

2.3.1 Peak seabed wave energy threshold analysis

According to the EUNIS classification scheme, a large area of the seabed around the UK is not disturbed by waves (the deep circalittoral and deep sea areas which fall at greater depths than the wave base), so the analysis of seabed kinetic energy caused by waves was restricted to shallower areas which are disturbed by waves (infralittoral and circalittoral). Two types of point data were used in the analysis, both extracted from the JNCC Marine Recorder database⁸: energy classified data points for infralittoral and circalittoral rock habitats and data points classified by wave exposure at sample sites.

Peak seabed wave energy categories from rock biotopes

EUNIS and the Marine habitat classification of Britain and Ireland split infralittoral and circalittoral rock habitat into high, moderate and low energy habitats. The distinction between wave and tidal energy in these classifications is not always explicit therefore each will be examined separately. Distribution data extracted from Marine Recorder for infralittoral and circalittoral rock biotopes were aggregated to their parent energy class (high, moderate or low energy).

The infralittoral and circalittoral rock data were in the form of point data from Marine Recorder (Table 2). Marine Recorder contains a field which classes records as certain or uncertain. Only records marked as 'Certain' were used in the analysis. Using the Hawth's Tool extension in ArcGIS 9.2, values from the peak seabed kinetic energy gridded raster layers (both waves and tides) were joined to the point shapefile containing habitat data. This resulted in a point file which contained infralittoral and circalittoral rock biotopes with their associated wave and current energy values according to the energy layers described in section 2.1 and 3.1. Any points with zero energy values were deleted. These occurred in areas where the gridded energy layer did not extend sufficiently close to the coast in many areas where habitats had been recorded

Circalittoral and infralittoral records were combined for each energy category. Energy values were log transformed before analysis. Descriptive statistics for each energy category were derived using Minitab v.15. Descriptive statistics included mean, standard deviation, variance, minimum, median, maximum, 1st and 3rd quartile values, confidence intervals and the Anderson Darling normality test.

⁸ The Marine Recorder package was developed by JNCC as a collect and collate piece of software designed to hold and manage marine survey data including Marine Nature Conservation Review surveys. The JNCC database holds benthic sample data from a variety of organisations including the JNCC, the Country Conservation Agencies, MEDIN, Seasearch and Local Record Centres

Table 2: High energy rock data points available from Marine Recorder

		No. of records		
		Certain	Uncertain	All
High energy	Circalittoral	1,515	470	1,985
	Infralittoral	1,859	686	2,545
Moderate energy	Circalittoral	1,453	567	2,020
	Infralittoral	2,555	674	3,329
Low energy	Circalittoral	283	87	370
	Infralittoral	1,225	324	1,549
	Total	8,890	2,808	11798

Wave exposure at sample sites

As well as biotope distribution data, Marine Recorder also includes qualitative information about the wave exposure at sites around the UK. These data are found in the Location table of the database and are displayed in Figure 9 - Figure 13. As part of the Marine Nature Conservation Review (MNCR) seven categories of wave exposure were identified and incorporated into field recording forms used to standardise survey data collection. Marine Recorder holds the results of surveys which have used these data forms; hence wave exposure data in Marine Recorder falls in these seven categories. The categories were based on the aspect of the coast (related to the direction of the prevailing or strong winds), fetch (distance to the nearest land), the degree of open water offshore and the depth of water adjacent to the coast (see Table 3). In Table 1 these wave exposure categories are grouped into their expected EUNIS energy class using expert judgement.

Table 3: MNCR wave exposure classes (Hiscock, 1996)

Wave Exposure	Description	Expected energy class
Extremely exposed	Open coastline, faces into prevailing winds & receives ocean swells for several 1000 kms and where deep water is close to the shore (50 m depth within 300m).	High
Very exposed	Open coastline, face away from prevailing winds & receives ocean swells for several 100 kms, where deep water is not close.	High
Exposed	Prevailing wind is onshore. Degree of shelter. Not generally exposed to strong or regular swell.	High
Moderately exposed	Open coast, facing away from prevailing winds, without long fetch but where strong winds can occur.	Moderate
Sheltered	Restricted fetch. Generally, face away from prevailing winds or have obstructions. Can face prevailing winds but with a short fetch	Low
Very sheltered	Unlikely to have fetch > 20 km. Face away from prevailing winds or have obstructions.	Low
Extremely sheltered	Sites fully enclosed with fetch no greater than 3 km.	Low
Ultra sheltered	Sites with fetch of a few tens or a several 100 ms.	Low

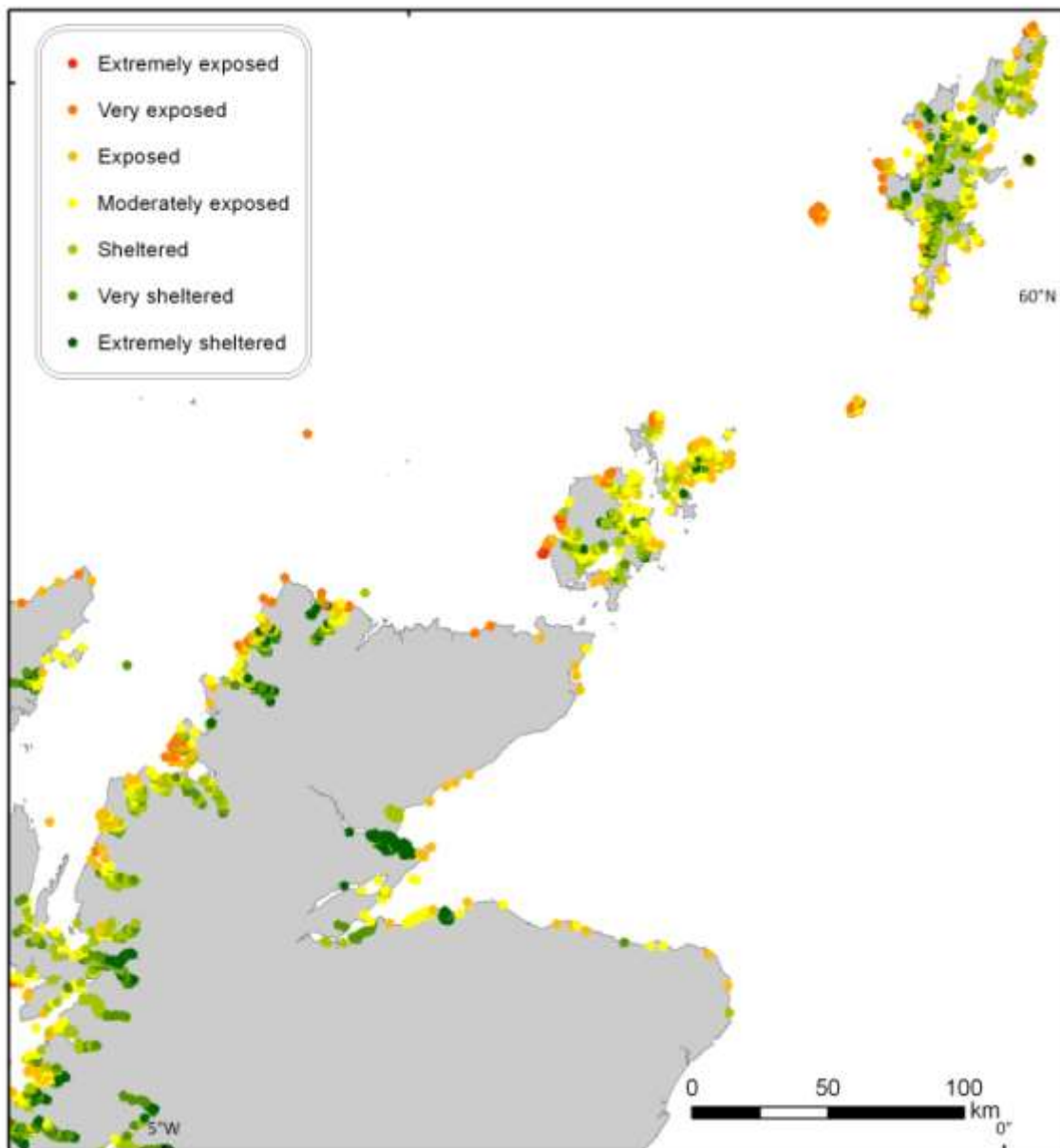


Figure 9: Wave exposure categories taken from the Location table in Marine Recorder for Orkney, Shetland and Northern Scotland.

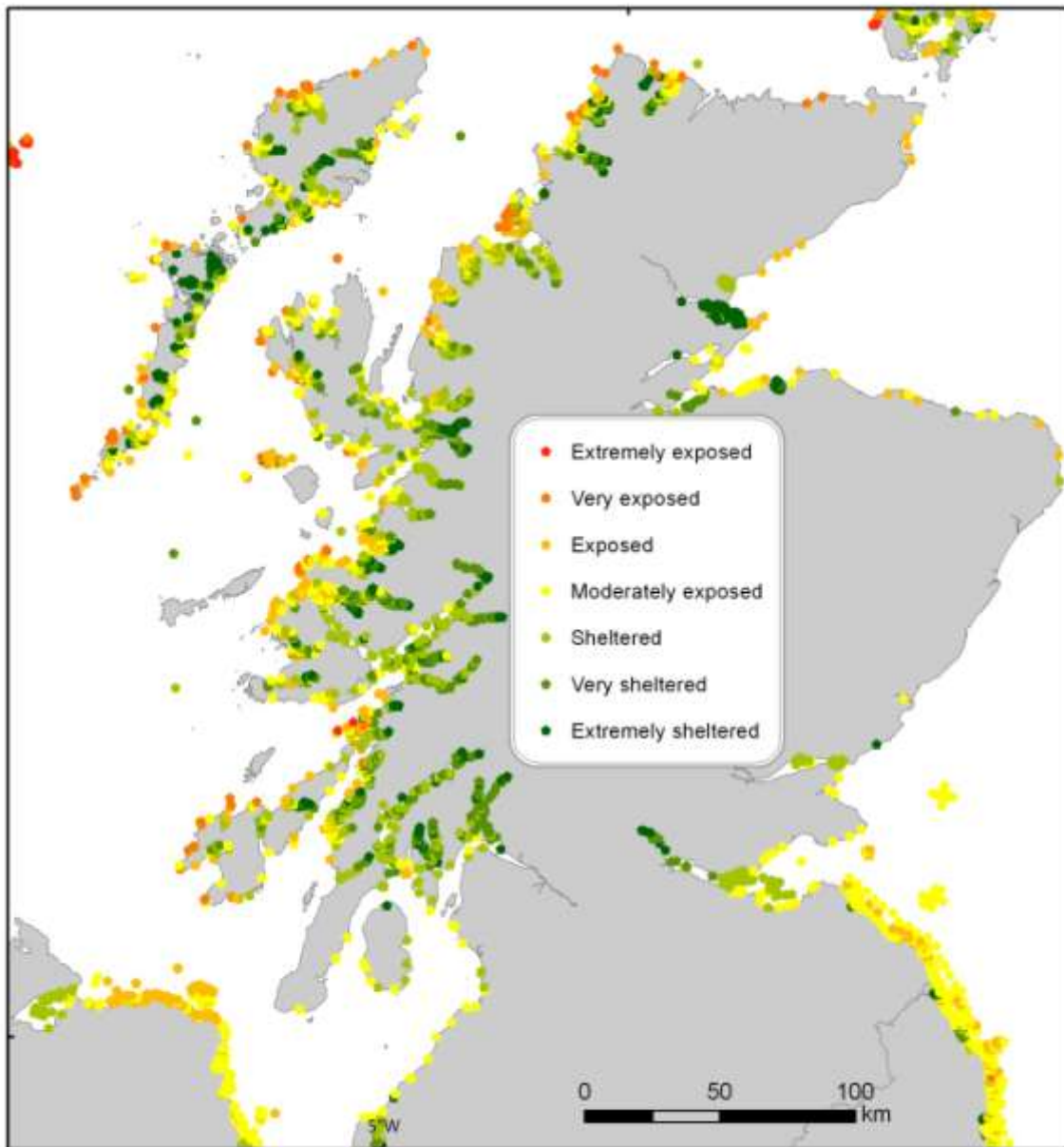


Figure 10: Wave exposure categories taken from the Location table in Marine Recorder for the Minches and western Scotland.

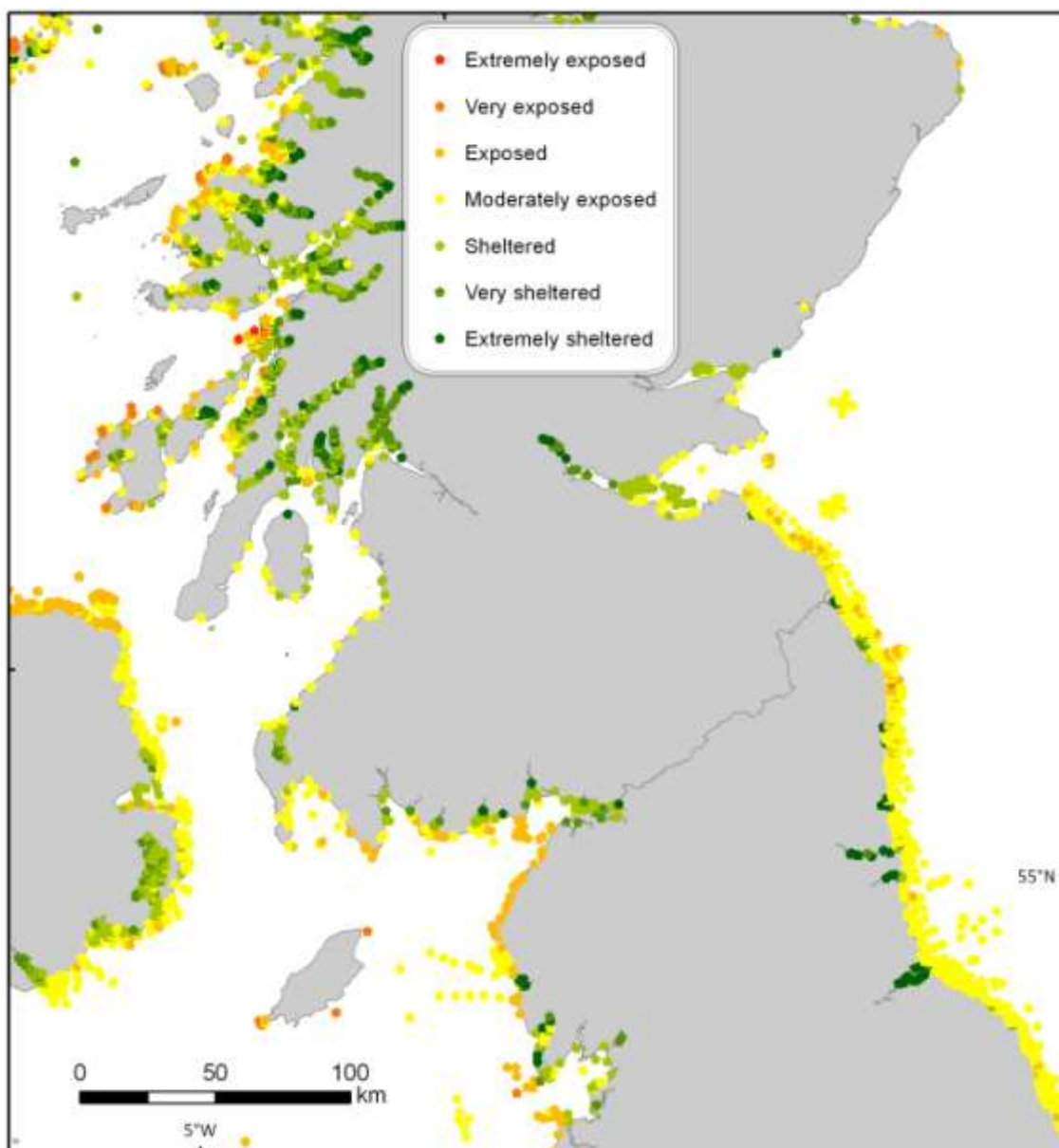


Figure 11: Wave exposure categories taken from the Location table in Marine Recorder of southern Scotland, northern England and Northern Ireland

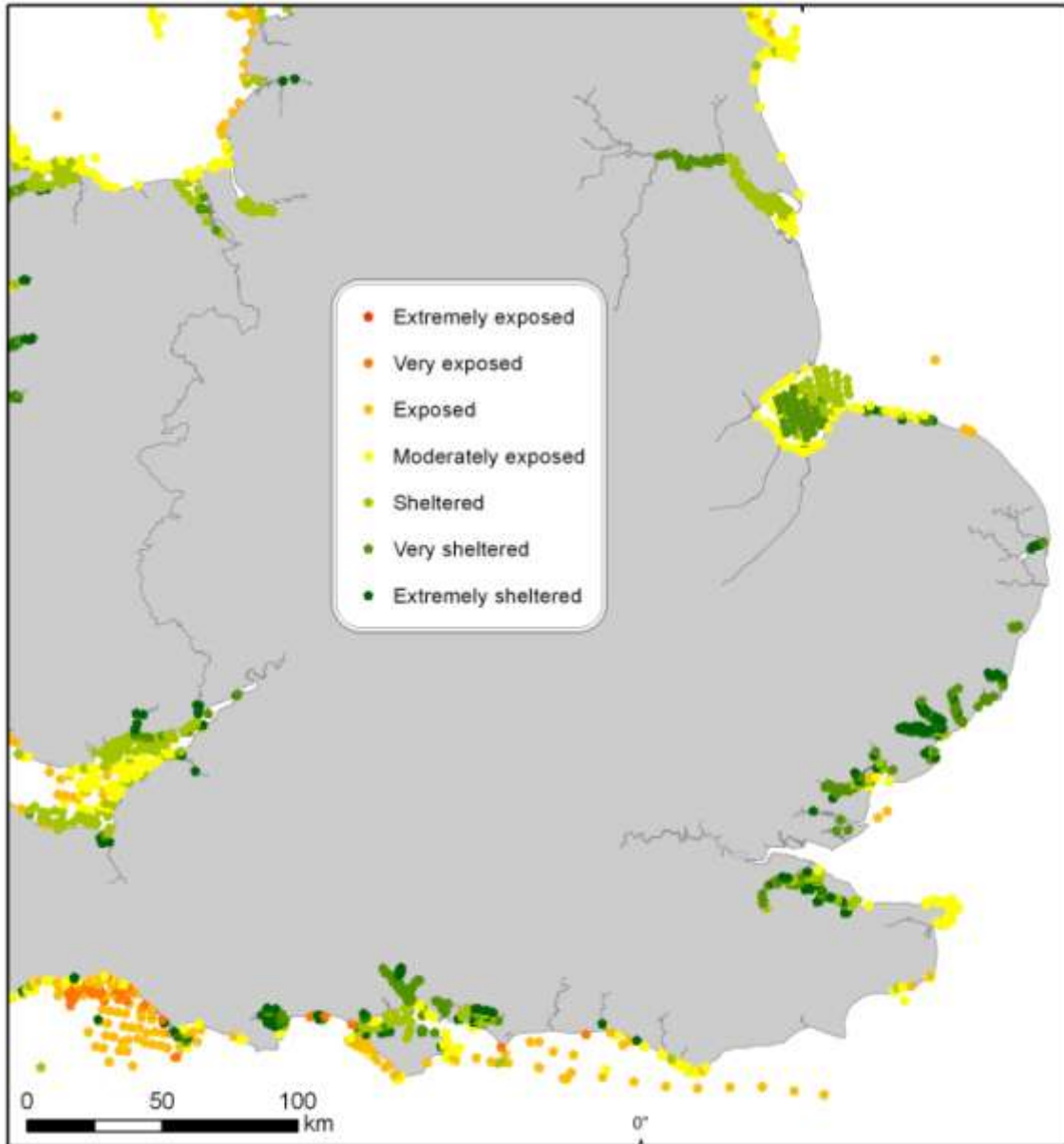


Figure 12: Wave exposure categories taken from the Location table in Marine Recorder for eastern and southern England.

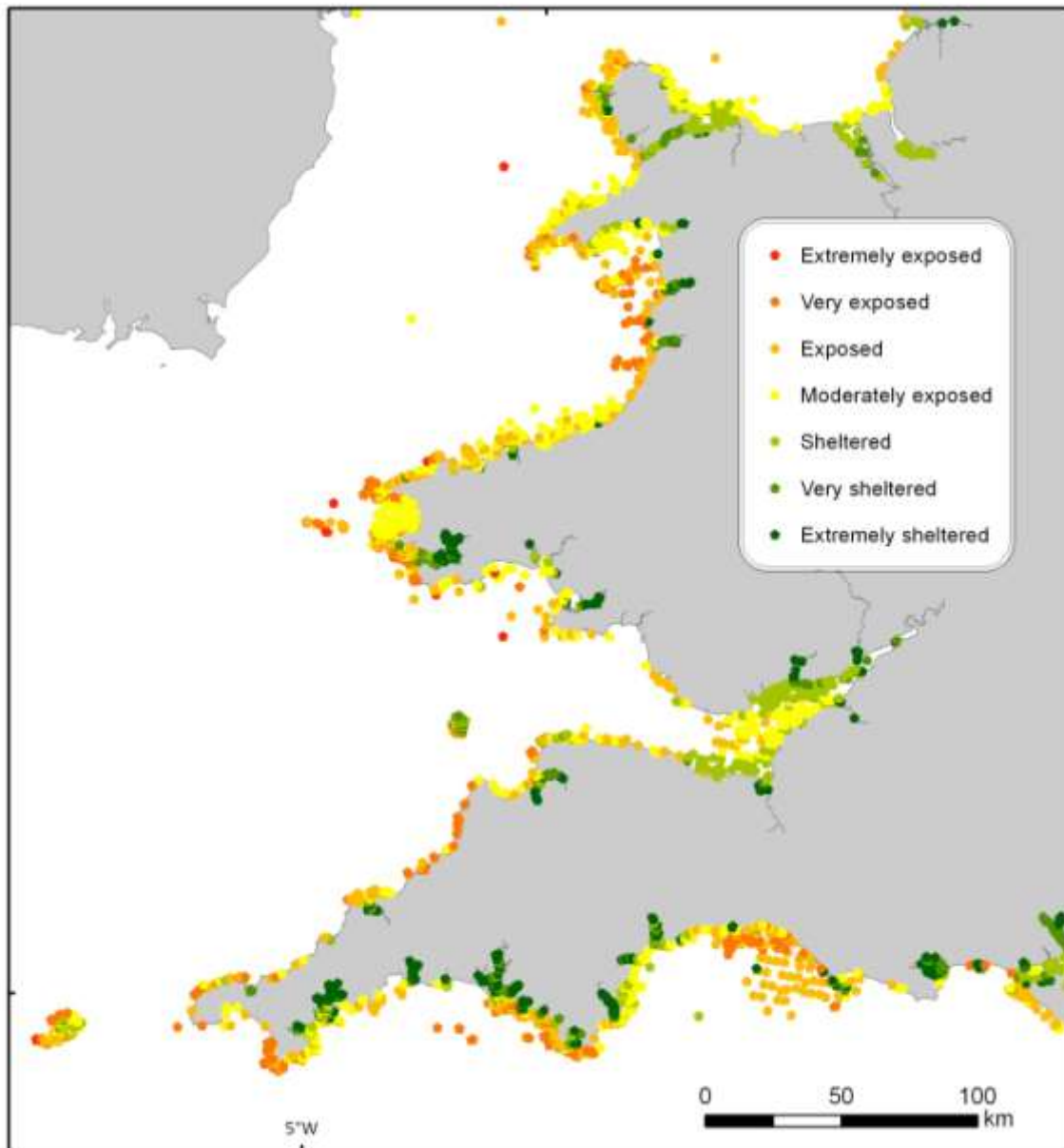


Figure 13: Wave exposure categories taken from the Location table in Marine Recorder of Wales and south-western England

The wave exposure data from Marine Recorder were in the form of point data (Table 4). Using the Hawth's Tool extension in ArcGIS 9.2, values from the peak seabed kinetic energy raster layers (both waves and tides) were joined to the wave exposure point shapefile. This resulted in a point shapefile which contained wave exposure data and their associated wave and current energy values according to the energy layers described in section 2.1 and 3.1. Any points with zero energy values for both peak seabed kinetic energy raster layers were deleted. These occurred in areas where the gridded energy layer did not extend sufficiently close to the coast in many areas where habitats had been recorded (as in section 2.2.1 in determining peak seabed wave energy)

Circalittoral and infralittoral records were combined for each wave exposure category. Wave exposure values were log transformed before analysis. Descriptive statistics for each energy

category were derived using Minitab v.15. These statistical outputs included mean, standard deviation, variance, minimum, median, maximum, 1st and 3rd quartile values, confidence intervals and the Anderson Darling normality test.

Table 4: Wave exposure data points available from Marine Recorder

Wave exposure	No. of records		
	Certain	Uncertain	All
Extremely exposed	1,651	228	1,879
Very exposed	3,198	619	3,817
Moderately exposed	10,326	2,252	12,578
Exposed	7,255	1,915	9,170
Sheltered	6,588	2,142	8,730
Very sheltered	3,640	1,138	4,778
Extremely sheltered	5,031	1,169	6,200
Total	37,689	9,463	47,152

Results

The range of values for peak seabed kinetic wave energy in the gridded raster layer seemed quite large (1 – 698 Nm⁻²). Table 5 shows the distribution of peak seabed kinetic energy due to wave values in the raster energy layer. It clearly shows that the majority of values range between 0 and 2 Nm⁻² in the first three categories (99.23%). Table 5 shows that the high values tend to be very few in numbers and are likely to be outliers in the model. The high values were determined to be likely to occur due to the mismatches between the resolution of the wave model and the bathymetry model in coastal areas.

Table 5: Count of the number of cells with peak seabed kinetic energy values due to waves.

VALUE (Nm ⁻²)	COUNT	VALUE (Nm ⁻²)	COUNT	VALUE (Nm ⁻²)	COUNT
0	13659059	23	8	108	2
1	616900	25	6	164	1
2	166597	26	6	174	1
3	55887	27	18	207	1
4	26886	28	8	211	2
5	16544	29	6	212	1
6	5817	30	13	213	3
7	2333	31	6	214	1
8	1231	32	2	215	5
9	615	35	1	216	6
10	337	37	1	273	2
11	196	44	2	285	2
12	116	45	1	366	2
13	52	46	3	375	2
14	38	47	2	438	1
15	44	48	1	446	1
16	16	50	2	524	4
17	27	53	2	535	3
18	16	56	2	536	4
19	11	57	3	537	1
20	4	68	1	538	2
21	9	82	2	698	2
22	13	106	1		

Peak seabed kinetic energy values were log transformed (\log_{10}) and descriptive statistics (Table 6) and 95% confidence intervals (Table 7) for the energy categories (derived from rock biotopes) were obtained. The thresholds were designated as the values which fell half way between the upper and lower confidence intervals for adjacent categories (Table 7). The threshold values were then anti-logged to obtain a value in Nm⁻².

Table 6: Descriptive statistics for the Marine Recorder biotope data points with high, moderate and low energy.

Descriptive statistics	High	Moderate	Low
Number	3220	3484	840
Mean	0.04921	-0.22263	-1.18280
Standard deviation	0.63284	0.78740	0.74870
Variance	0.40049	0.62000	0.56060
Min	-2.00000	-2.00000	-2.00000
1st quartile	-0.20761	-0.67780	-2.00000
Median	0.19033	0.40951	-1.30100
3rd quartile	0.48144	0.40951	-0.06383
Max	1.34811	1.34811	1.03860

Table 7: 95% Confidence intervals for log transformed seabed kinetic wave energy data.

Energy category	Number of points	Upper confidence interval of the median	Lower confidence interval of the median
High	3220	0.21484	0.16435
Moderate	3484	-0.00436	-0.06550
Low	840	-1.3010	-1.3979

Figure 14 shows peak seabed kinetic energy caused by waves split into high, moderate and low energy classes using the energy classes derived from biotope point data. Areas of high energy appear off the west coast of Scotland; west of the Hebrides, Orkney and Shetland Islands, on the Dogger bank, above the Wash, Cardigan Bay and the South of England. Low wave energy areas mainly appear to the east of the Hebrides and in the complex coastline of western Scotland as well as other sheltered or deeper areas around the coast.

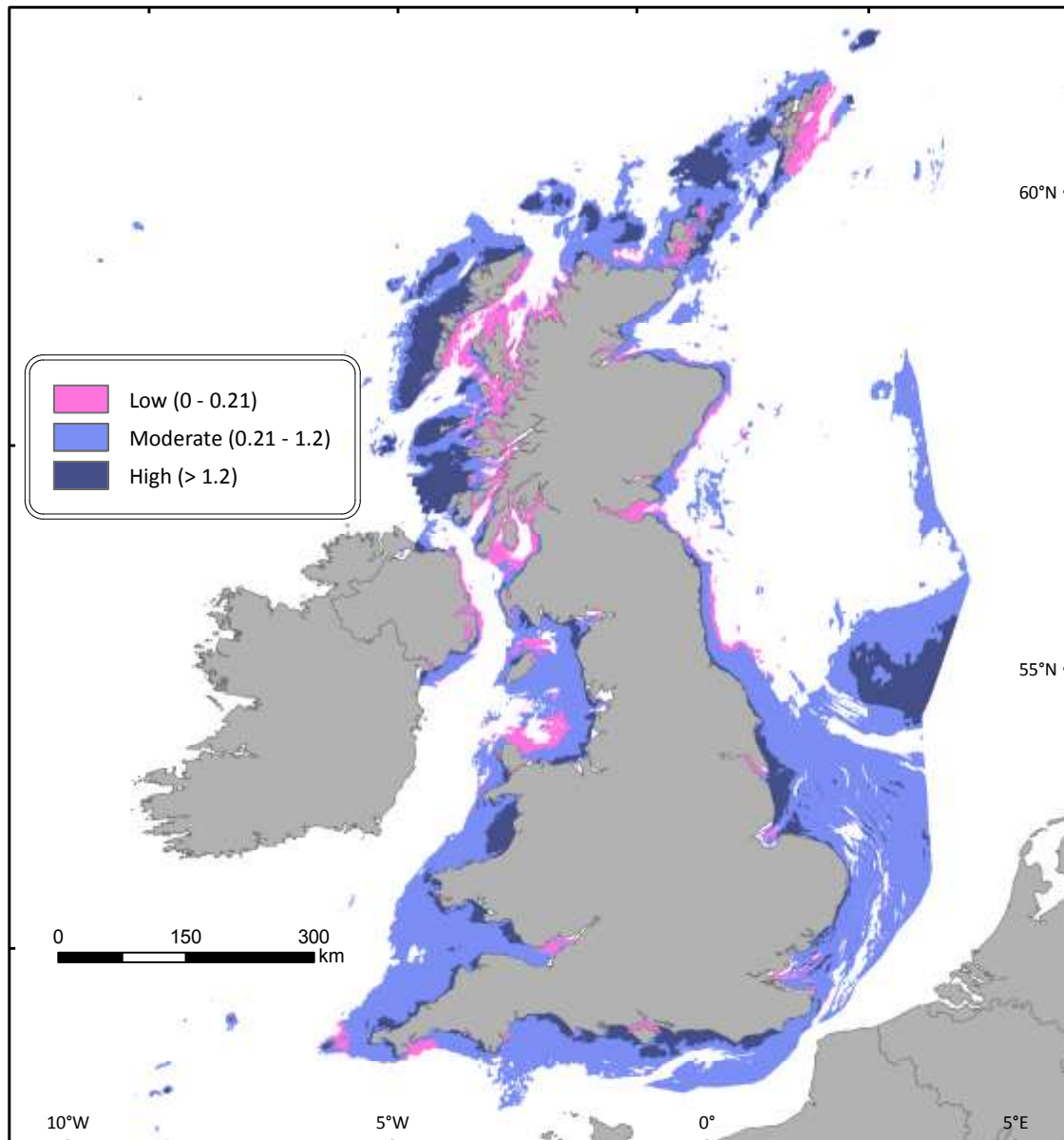


Figure 14: Peak seabed wave kinetic energy (Nm^{-2})

Point data with associated wave exposure classes were spatially joined to the energy classes in Figure 14. Table 8 shows the number of wave exposure points associated with each energy class. For each energy class, the proportions of wave exposure data falling in each wave exposure category are given as percentages in Figure 15. Extremely exposed, very exposed and exposed sites comprise 62% of the records in the high energy class. The moderate energy class is dominated by moderately exposed habitats (49%). The low energy class is dominated more by sheltered, very sheltered and ultra sheltered locations (72%). These values are used as performance rating scores in the seabed kinetic energy confidence section. Extremely and very exposed categories would be expected to dominate the high energy class, while sheltered categories would be expected to dominate the low energy classes.

Table 8: Number of points in each energy and wave exposure category ES = extremely sheltered, VS = Very sheltered, S = Sheltered, ME = Moderately exposed, E = Exposed, VE = Very exposed and EE = extremely exposed

Energy	Wave Exposure							Total
	ES	VS	S	ME	E	VE	EE	
High	30	64	201	1069	1259	747	162	3532
Moderate	66	116	375	1492	860	154	9	3072
Low	604	312	697	484	130	16		2243
Total	700	492	1273	3045	2249	917	171	8847

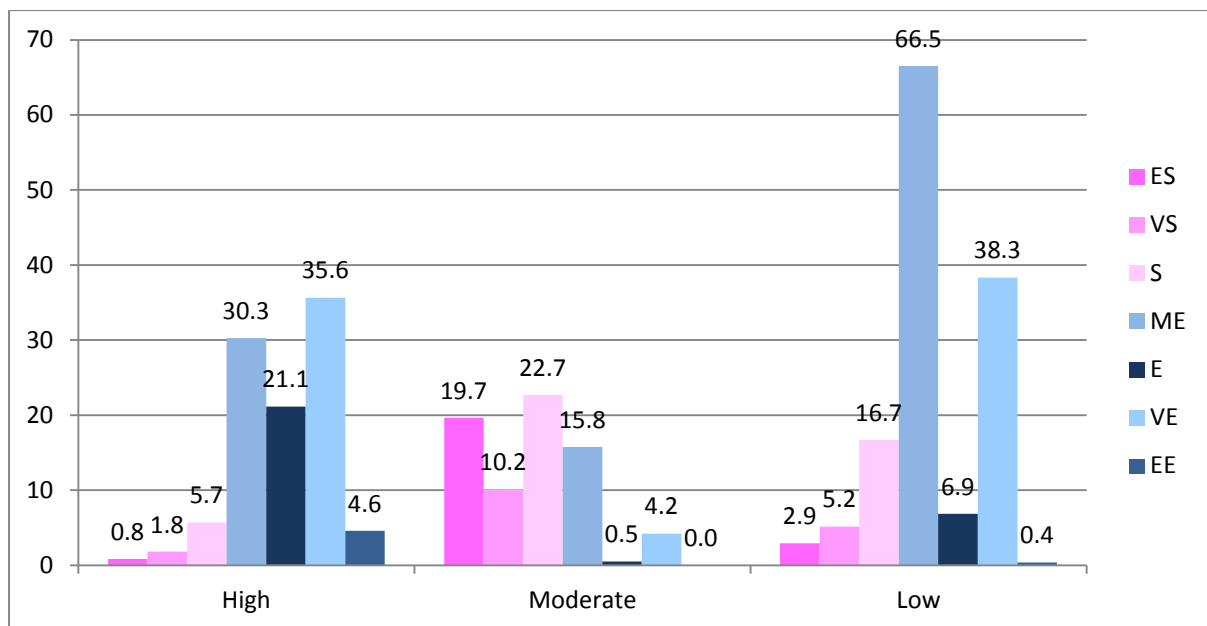


Figure 15: The relationship between energy class and wave exposure categories, shown as the percentage of sites located in each energy class (as shown in Figure 11) which have a particular wave exposure. ES = extremely sheltered, VS = Very sheltered, S = Sheltered, ME = Moderately exposed, E = Exposed, VE = Very exposed and EE = extremely exposed.

A chi-square test of association was performed to test whether the exposure categories within the energy classes differed from each other (see Table 9). As the wave exposure classes were assigned to energy classes using expert judgement, chi square tests were used to validate whether the exposure classes were placed within the right energy categories. The null hypothesis that the energy class (derived from analysis with biotope data) is independent from wave exposure (site data points) is rejected ($\chi^2 = 2807$, DF = 4, P < 0.05). For the high energy rock class, values for exposed locations were higher than expected and for sheltered locations were lower than expected if the energy categories were independent of wave exposure. The low energy rock class had lower than expected values for exposed locations and higher than expected values for sheltered locations. Relatively small differences were observed between actual and expected values in moderate energy environments.

Table 9: Chi-Square test of association for wave exposure categories within rock energy classes ($\chi^2 = 2807$, DF = 4, P < 0.01).

	Wave Exposure		Exposed	Moderately exposed	Sheltered	Total
Energy	High	Actual	2347	1746	359	4452
		Expected	1679	1532	1240	
	Moderate	Actual	735	809	543	2087
		Expected	787	718	581	
	Low	Actual	255	490	1563	2308
		Expected	871	794	643	
Total		3337	3045	2465	8847	

2.3.2 Seabed kinetic wave energy confidence

An assessment of the confidence in the seabed kinetic energy wave model was made by comparing values of wave height and wave period output from NOC ProWAM against simultaneous wave buoy data gathered by Cefas (West *et al*, 2010). This provided a mean and standard deviation of the differences between the Cefas data and the NOC ProWAM predictions of wave height and period. These statistics were combined with the standard deviations of water depths to derive a probability layer for the peak wave-induced water particle velocity (West *et al*, 2010).

The probability layer for the peak wave-induced water particle velocity was combined with information about the probability of being in the right energy class. The energy classes established through the threshold testing of the boundaries between high, moderate and low energy in section 2.3.1 each had a performance rating. The performance rating used the percentage of wave exposure points (exposed, moderately exposed or sheltered) which fell into in the expected energy class (high, moderate or low). The levels of uncertainty associated with the three classes of energy, due to corresponding uncertainty in wave height, period and water depth, were obtained by integrating the probability of peak wave-induced water particle velocity over the appropriate range for each class. The result was a set of three class-related probabilities (West *et al*, 2010).

The final stage was to multiply each probability by the performance rating for each class and then to take the class possessing the highest overall probability value, as the most probable class. Maps were then produced showing the most probable class for each model cell, accompanied by the associated probability or confidence level.

3 Tidal currents

3.1 Tidal current models

The tidal current energy layers came from NOC current models (CS20, CS3 and NEA models which cover different parts of the UK marine area (Table 10 and Figure 16).

Table 10: Description of the tidal current models used in UKSeaMap 2010.

	Resolution (km)	Description
High resolution Continental Shelf Model (CS20)	1.8	The HRCS model is run 11 of the 3D model (ABPmer, 2008). It occurs with the 200m depth contour and tidal data available at 32 sigma levels through depth. Data has been included from 5 layers: the 50% layer and then at 10% intervals towards the bed, areas where large variation in flows due to near bed effects.
Continental Shelf Model (CS3/CS3X)	12	The model is two dimensional and uses up to 26 tidal harmonic constants to provide tidal elevation together with current speed and direction at six different depths (sigma levels) deduced from the depth-averaged currents using a set of vertical current profiles. The six sigma levels for the currents are at the depths 0% (surface), 25%, 50% (mid-depth), 75%, 90% (near-bottom) and 100% (bottom) (ABPmer, 2004).
North East Atlantic Model (NEA)	35	The model is two dimensional providing depth-average parameters (ABPmer, 2004).

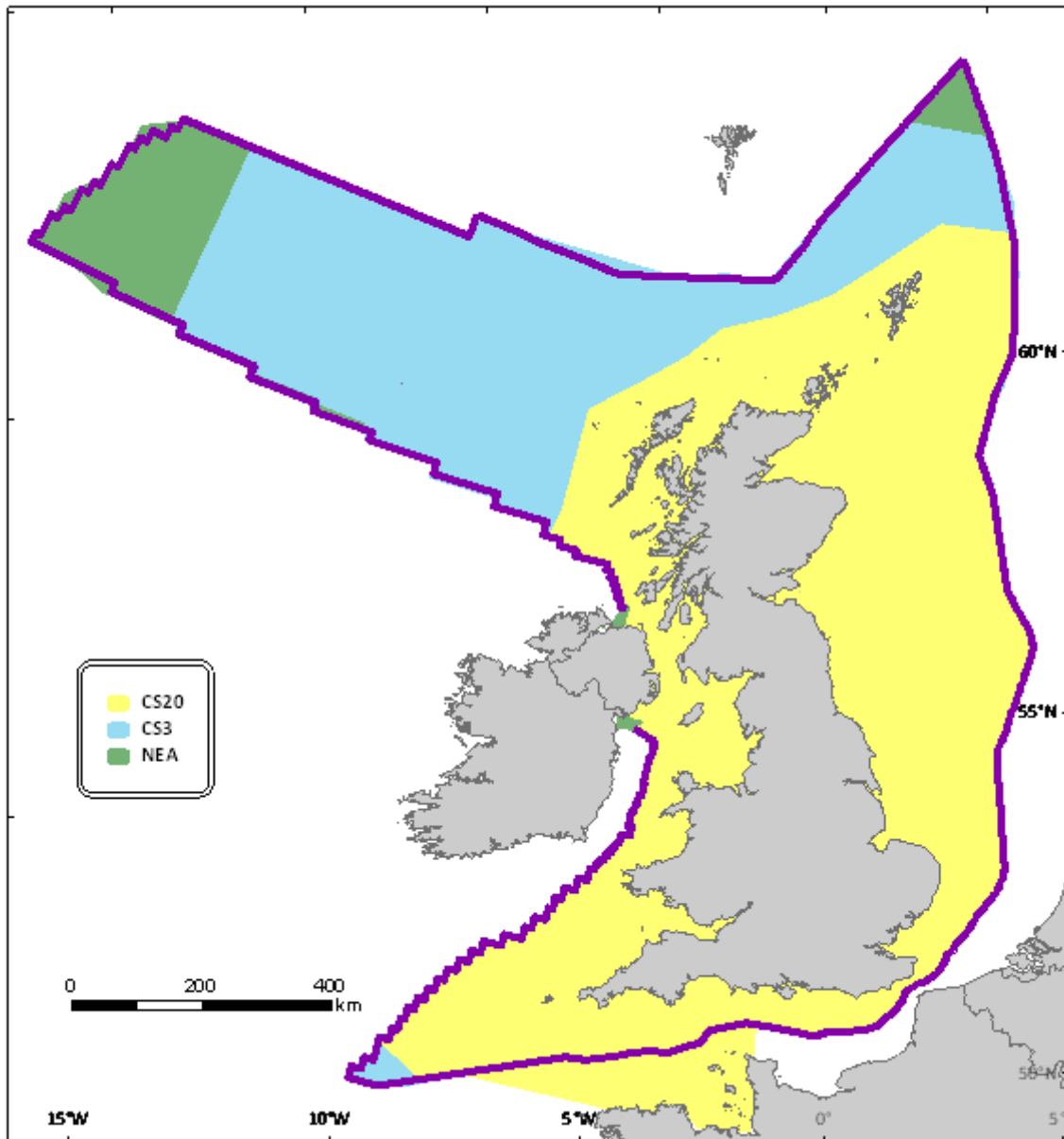


Figure 16: Extent of tidal models.

3.2 Seabed kinetic current energy threshold analysis

The aim of this work was to split seabed current kinetic energy layer into the three EUNIS energy categories: high, moderate and low. These categories are applied to rock habitats only in the littoral (not considered as part of UKSeaMap 2010), infralittoral and circalittoral zones. Several options were considered and habitat point data from the Marine Recorder database were used to attempt to validate the energy categories by either using tidal stream data points (very strong – very weak tidal streams) or by using the circalittoral and infralittoral high, moderate and low energy categories (derived from habitat descriptions). Both of these efforts overestimated the amount of high tidal energy and produced unsatisfactory results. In the former case this is likely to be due to the fact that the point data is on a much finer scale than the gridded kinetic energy data (300m). In the latter case, this

is most likely because the energy categories are a combination of wave and tidal current energy and usually by waves rather than tides. Instead the categories were divided using the MNCR current speed values devised by Hiscock (1996).

Hiscock (1996) divides tidal streams into five categories: very strong, strong, moderately strong, weak and very weak (Table 11). The category values were converted from tidal current speed (ms^{-1}) to peak seabed kinetic tidal current energy (Nm^{-2}) (Figure 17). To equate these tidal stream categories with the three energy categories in the EUNIS classification, very strong and strong tidal streams were combined into the high energy category and weak and very weak tidal streams were combined to represent low energy environments. There were very few areas in the map showing very strong tidal streams, the most obvious being the Pentland Firth, (Figure 17). As Hiscock (1996) did not define a value for the boundary between weak and very weak tidal streams these were combined to represent low energy.

Table 11: MNCR tidal stream categories.

Surface Tidal Streams	Speed (Knots)	Speed (ms^{-1})	Kinetic Energy (Nm^{-2})	EUNIS energy category
Very strong	>6	>3	> 4.5	High
Strong	3 – 6	1.5 – 3	1.16 – 4.5	High
Moderately strong	1 – 3	0.5 – 1.5	0.13 – 1.16	Moderate
Weak	< 1	< 0.5	<0.13	Low
Very weak	Negligible	Negligible	Negligible	Low

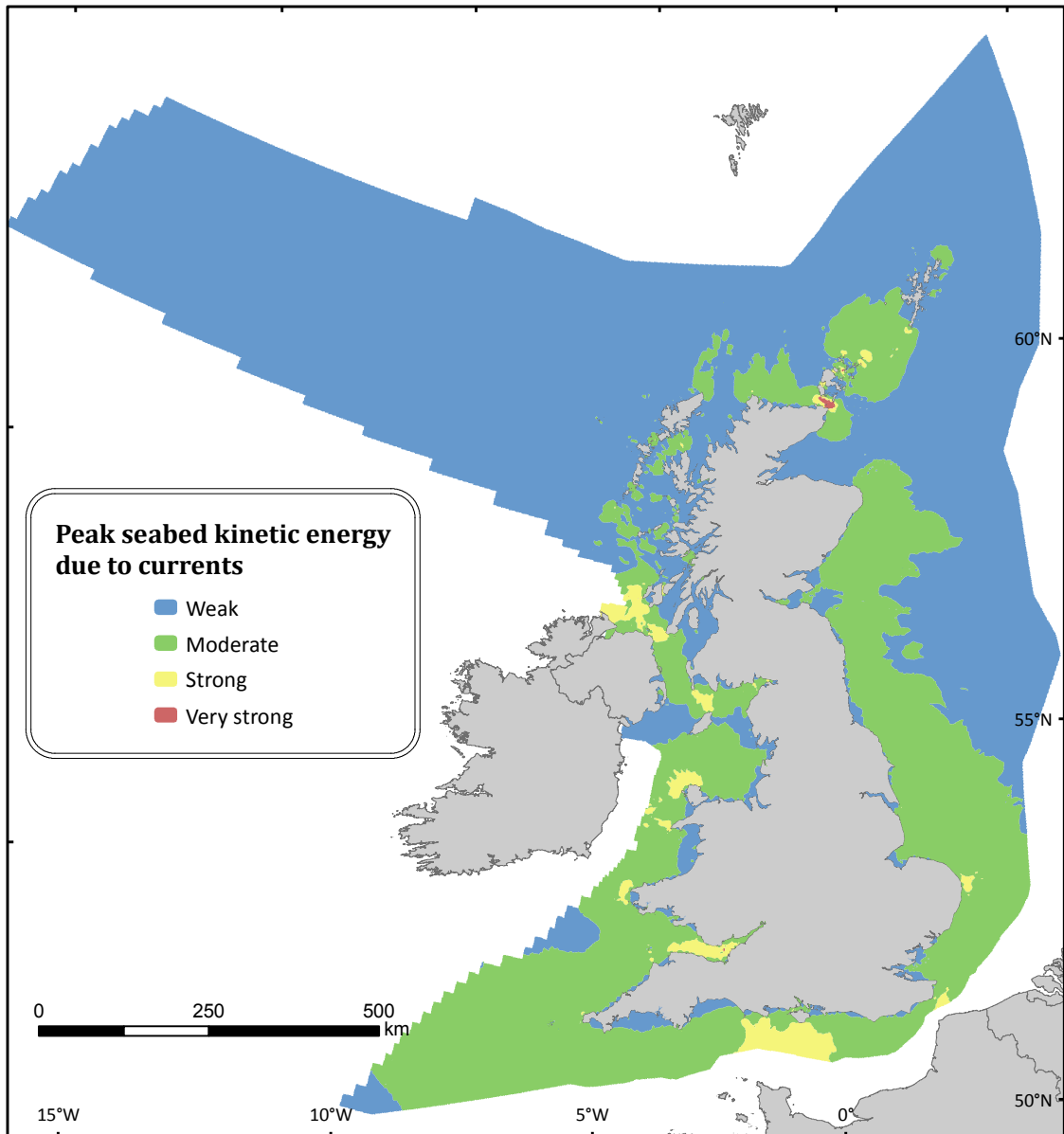


Figure 17: Classified map of peak seabed kinetic energy due to currents (for units see Table 11).

3.3 Current energy confidence

The ideal method for calculating probabilities for peak seabed current energy would use differences between peak predicted values and peak observed values for current speeds (West *et al*, 2010). The observed data are freely available from the British Oceanographic Data Centre (BODC). This project did not have the resources (within the required timescales for completion of the project), to obtain the corresponding predicted data values from NOC from the same location and time as the observed data. Values from Holt *et al*, (2005) which reviewed error quantification were used instead. This was not ideal and is likely to lead to an over-estimation of confidence in the current models.

Using harmonic analysis, Holt *et al*, (2005) reported the mean and the Root Mean Square (RMS) errors from a comparison with harmonic analyses of historical data around the NOCCOMS model area. Holt *et al*, (2005) gave error values for the first six harmonic constituents. It was then assumed that the errors for each harmonic constituent followed a normal distribution and that sum of all the harmonic constituents is also a normal distribution. The six constituents quoted by Holt *et al*, (2005) together represent approximately 85% of the total tidal current generating value). It was assumed that the total mean error was given by the sum of the mean errors attributed to each of the six harmonic constituents and that the total variance was the sum of the six individual contributions (West *et al*, 2010). It was assumed that the uncertainty in the modelling results led to a normal probability distribution for current speed, using the mean and standard deviation values for the six constituents (West *et al*, 2010).

The boundaries of the high, moderate and low energy classes were identified in Table 11. The probability of a model cell falling into each class was obtained through integration of the probability density over the ranges of the three classes. The most likely class was then taken as the class with the highest probability value (West *et al*, 2010). The uncertainty in the peak seabed kinetic current energy layer was calculated by subtracting the probability from 1.0.

4 Combined energy layer

Energy classes in EUNIS are not split into separate wave and tidal current energy classes. A single energy layer splitting energy into high moderate and low energy classes was required to model EUNIS Level 3 rock habitats. Wave and current energy classes were combined using rules in the energy matrix (Table 12) and applied to UK seas in Figure 18. The highest category was selected in each case, e.g. high wave and moderate current would result in a high energy category, and a low wave and moderate current combination would result in a moderate energy category. This approach was used as current and waves act on the seabed in different ways. It is not possible to distinguish the combined effect of wave energy and current energy by adding the models numerically.

Table 12: UKSeaMap 2010 energy matrix

Wave energy	Current energy		
	High	Moderate	Low
High	High	High	High
Moderate	High	Moderate	Moderate
Low	High	Moderate	Low

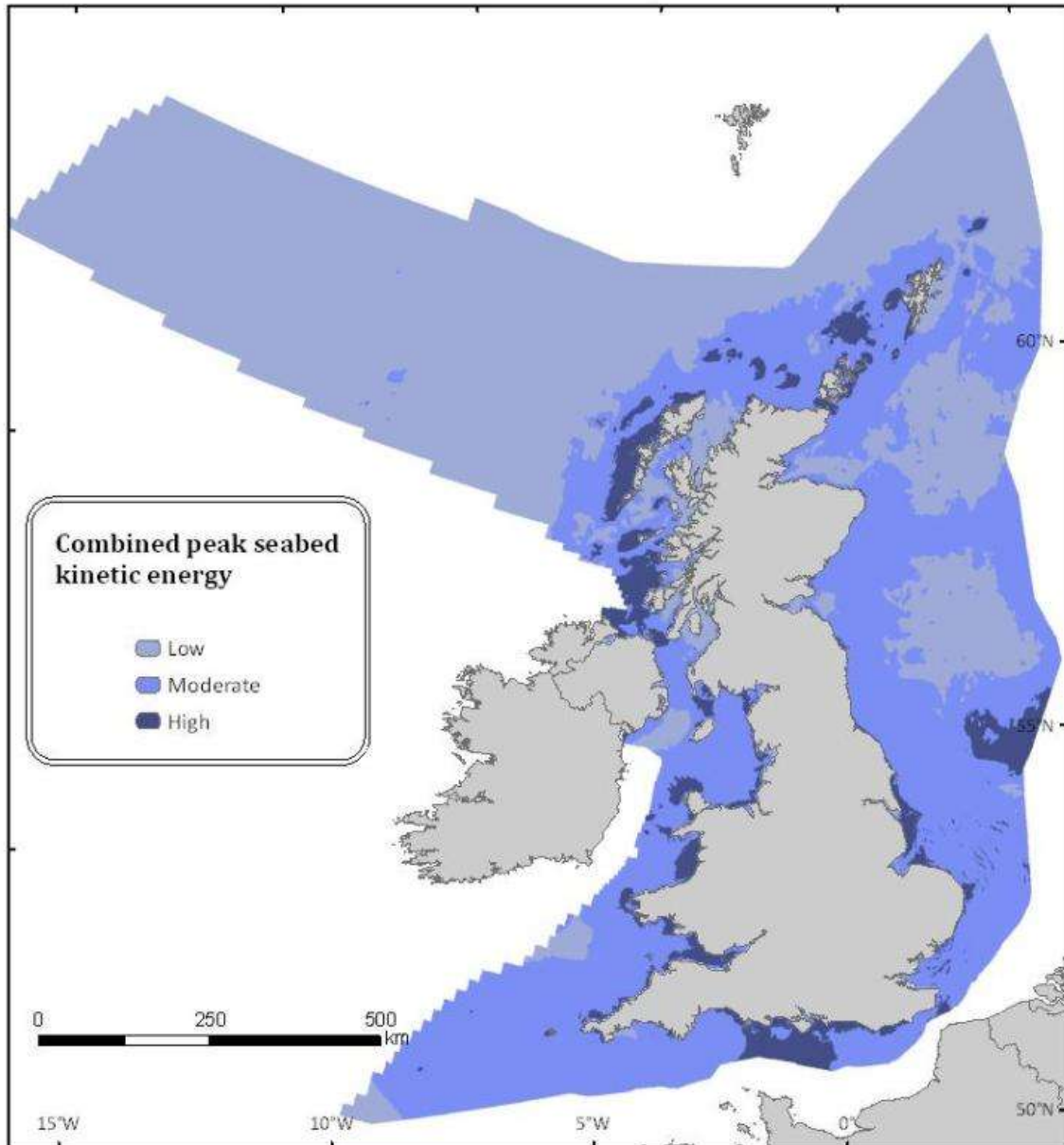


Figure 18: Classified map of combined peak seabed kinetic energy (due to both waves and currents).

5 Conclusions

Energy data were used to predict EUNIS energy classes of high, moderate and low for infralittoral and circalittoral rock habitats. Analysis of energy datasets included peak water velocities, kinetic energy and shear bed stress data due to both currents and waves. Peak seabed kinetic energy was selected as the most suitable parameter to predict EUNIS energy classes for both the wave and current datasets.

There was a high amount of variance in the data (see Table 6) from Marine Recorder, making it difficult to delineate thresholds. From the subsequent wave exposure analysis and chi square tests the chosen categories appear to be best for high energy, followed by low and moderate energy categories. It is recommended that these thresholds be revised in the

future when more habitat data becomes available. The UKSeaMap 2010 Technical Report No. 5 (Ellwood *et al*, 2011) (compares EUNIS energy classes from habitat maps from survey data with the energy classes from UKSeaMap 2010. A good match was obtained between the energy classes (~60%) but the survey maps used in the analysis only cover 6% of the seabed. It would be useful to repeat this analysis when more detailed infralittoral and circalittoral survey habitat maps become available.

Appendix: Version Control

Build status:

Version	Date	Author	Reason/Comments	Sections
0.1	11/03/2010	Fionnuala McBreen	1st draft	
0.2	16/11/2011	Fionnuala McBreen	Incorporating comments from Natalie Askew and Andy Cameron	
0.3	05/12/2011	Fionnuala McBreen	Incorporating comments from Dan Bayley	

Reference List

- ABP MARINE ENVIRONMENTAL RESEARCH LTD, 2004. Atlas of UK Marine Renewable Energy Resources: Technical Report.
- ABP MARINE ENVIRONMENTAL RESEARCH LTD, 2008. Atlas of UK Marine Renewable Energy Resources: Technical Report.
- ELLWOOD, H., MCBREEN, F. & ASKEW, N., 2011. UKSeaMap 2010 Technical Report 5: Analysing the relationship between substrate and energy data.
- FROST, N. J., PETREY, D., & SWIFT, R. H., 2010. Accessing and developing the required biophysical datasets and datalayers for Marine Protected Areas network planning and wider marine spatial planning purposes: Report No.1: Task 1C. Assessing the confidence of broad scale classification maps.
- HISCOCK, K (ed). 1996. *Marine Nature Conservation Review: rationale and methods*. Joint Nature Conservation Committee: Peterborough.
- HOLT, J., ALLEN, J. I., PROCTOR, R., & GILBERT, F., 2005. Error quantification of a high-resolution coupled hydrodynamic-ecosystem coastal-ocean model: Part 1 model overview and assessment of the hydrodynamics. *Journal of Marine Systems*, **57**, 167 - 188
- SOULSBY, R. 1997. *Dynamics of marine sands: a manual for practical applications*. Thomas Telford:
- WEST, N., SWIFT, R., & BELL, C., 2010. Accessing and developing the required biophysical datasets and data layers for Marine Protected Areas network planning and wider marine spatial planning purposes: Report No 10: Task 2E. Models of Fetch and Wave Exposure.